Journal of Polymer Research (2019) 26: 235
https://doi.org/10.1007/s10965-019-1870-x

ORIGINAL PAPER

Kinetics and thermodynamics of adsorption of Cu^{2+} and methylene blue to casein hydrogels

Juzhen Yi[1] · Yongqiu Li[1] · Liqun Yang[1] · Li-Ming Zhang[2]

Received: 15 January 2019 / Accepted: 23 July 2019 / Published online: 28 August 2019

Abstract

Several casein hydrogels were synthesized using glutaraldehyde as a crosslinker. The hydrogel prepared from 10 wt% casein and 5 wt% glutaraldehyde at pH = 7.5 showed the best adsorption performance for Cu^{2+} and methylene blue (MB). The morphology and thermal stability of the hydrogels were characterized by Fourier transform infrared spectrophotometry (FTIR), field emission scanning electron microscopy (FESEM) and thermo gravimetric analysis (TGA). Adsorption data were observed to fit well to pseudo second-order kinetics and the Freundlich-Langmuir switch model. The thermodynamic parameters of the adsorption showed that the adsorption of Cu^{2+} and MB into casein hydrogel was a spontaneous process.

Keywords Casein hydrogel · Adsorption kinetics · Thermodynamics · Methylene blue · Copper ions

Introduction

Industrial wastewater is a major source of heavy metals, dyes, and other organic pollutants in water supplies. These pollutants are found in the industrial waste streams associated with the manufacture of batteries, dyes, textiles, paper, and paints [1]. The high levels of these pollutants in wastewater is a serious global environmental issue and many pollutants in developed and developing countries are harmful to both human and animal life [2, 3]. The removal of pollutants from industrial wastewater has drawn considerable interest. Adsorption methods are highly effective and economical processes for removing metals, dyes, and organic pollutants from industrial effluents. Recent studies have established that natural materials are effective adsorbents owing to their ability to eliminate a wide range of pollutants, ready availability, eco-friendly nature, and low cost [4, 5]. Particular attention has been paid to superabsorbent hydrogels (SAH), which are three-dimensional cross-linked polymer networks of flexible chains [6]. The high water content and network structure allow solute diffusion through the hydrogel structure. Because SAH hydrogels possess ionic functional groups, they can absorb and trap ions and ionic dyes, such as Cu^{2+} and methylene blue (MB), from wastewater. As an important type of biopolymer, caseins are phosphoproteins that precipitate from raw skimmed milk by acidification with molecular weights in the range from 19 to 25 kDa [7]. More than 55% of the amino acids in casein proteins contain hydrophilic functional groups, such as -COOH, $-NH_2$, and –OH [8]. These molecules also possess favorable characteristics suitable for the development of hydrogel adsorption materials, such as high hydrophilicity, good biodegradability, and high performance in binding ions and small molecules, and exceptional surface-active and stabilizing properties. Moreover, these materials are less expensive and more readily available compared with collagen [9], silk fibroin [10], bovine serum albumin [11], and elastin-like polypeptides [12], which are usually used to prepare protein-based hydrogels. Casein hydrogels have been reported to be promising

Electronic supplementary material The online version of this article (https://doi.org/10.1007/s10965-019-1870-x) contains supplementary material, which is available to authorized users.

✉ Juzhen Yi
cesyjz@mail.sysu.edu.cn

[1] Department of Polymer and Material Science, School of Chemistry, Key Laboratory for Polymeric Composite and Functional Materials of Ministry of Education, Guangdong Provincial Key Laboratory for High Performance Polymer-based Composites, Sun Yat-Sen University, Guangzhou 510275, China

[2] School of Materials Science and Engineering, Sun Yat-Sen University, Guangzhou 510275, China

biomaterials in a recent study of their bifunctionality [13–15]. However, few studies have examined the kinetic and thermodynamic features of the adsorption of heavy metals and dyes onto casein hydrogels.

Experimental

Materials

Casein powder was purchased from Lanzhou Tongjian Biotechnology Co. (China); it was made from Yak milk with high quality. Glutaraldehyde (25% aqueous solution) was obtained from Guangzhou Guanghua Chemical Co. (China). All other chemicals and reagents, including $CuSO_4$, methylene blue and NaOH, were of analytical grade and used as the received. Double distilled water was used for the crosslinking and adsorption experiments.

Preparation of casein hydrogels

The hydrogels were synthesized in a three-necked reactor at 50 °C for 4 h. The reactor was fitted with a stirrer, a thermometer pocket and a condenser. To prepare the casein gel, aqueous casein solution was first prepared by dissolving casein powder in distilled water, and its pH value was then adjusted to be approximately 8 with 2.0 mol/L of sodium hydroxide solution. Specified amounts of casein solution and glutaraldehyde were then added to the reactor, which was placed in a constant temperature bath. The temperature of the reaction mixture was raised to 50 °C and the reaction was continued for 4 h. After the formation of a dark brown gel, the reaction mixture was cooled to ambient temperature. The resulting gel was washed with distilled water several times and then freeze-dried to a constant weight. Two series of hydrogels were prepared by varying the contents of casein (8.0, 10.0, 12.0, and 14.0 wt%) with a fixed 5 wt% of crosslinker (glutaraldehyde) and varied crosslinker concentration (2.5, 3.5, 5.0, and 10.0 wt%) with a fixed 10 wt% of casein.

Characterization of the hydrogels

The various hydrogels were characterized by FTIR using KBr pellet made by mixing KBr with fine powder of the polymer gel samples. The surface morphology of the hydrogels was characterized by FESEM (model JSM-6330F, made by JEOL company of Japan). Thermal stability of the hydrogels were evaluated by TGA in a Perkin Elmer instrument (USA) in nitrogen atmosphere at the scanning rate of 10 °C per minute in the temperature range of RT–900 °C.

Cu^{2+} and MB dye adsorption kinetics

The adsorption of Cu^{2+} and MB into the hydrogels depends on the physical and chemical interactions between adsorbates and hydrogel adsorbent, as well as transport of Cu^{2+} and MB from bulk solution to the hydrogel surface. The mechanism of adsorption can be evaluated in terms of adsorption kinetics by measuring the adsorption at various time intervals (q_t) till equilibrium (q_e) for a fixed initial feed concentration of Cu^{2+} or MB (C_i). However, the application of a single kinetic model is not sufficient to explain the heterogeneous nature of the adsorbent surfaces and also the diversity of adsorption processes. The term 'pseudo' is used for first and second order rate constant because of their dependence on initial dye concentration [16]. In the present system Cu^{2+} and MB adsorption data were not found to give good fits to pseudo 1st order rate kinetics (Eq. (1)), but did give good fits to pseudo second order rate kinetics (Eq. (2)) [17]. For evaluating the diffusion mechanism of Cu^{2+} and MB adsorption, the intra particle diffusion model (Eq. (3)) of Weber and Morris [18] was also used:

$$\frac{1}{q_t} = \left(\frac{k_1}{q_1}\right)\left(\frac{1}{t}\right) + \frac{1}{q_1} \tag{1}$$

$$\frac{t}{q_t} = \frac{1}{k_2 q_2^2} + \left(\frac{1}{q_2}\right)t \tag{2}$$

$$q_t = k_p t^{1/2} + C \tag{3}$$

In Eqs. 1–3, k_1 and k_2 are pseudo first and second order rate constants, q_1 and q_2 are the adsorption capacities at equilibrium, k_p is the rate constant for intra particle diffusion, and C is the intercept which signifies boundary layer resistance.

Desorption of Cu^{2+} and MB was performed with portions of 10 mL 0.1 M HCl for 1 hour. The treatment was repeated until total desorption of metal cation and MB were reached. The regeneration was performed with 0.1 M NaOH for 1 hour, followed by washing to neutral pH.

Cu^{2+} and MB adsorption isotherms

Adsorption isotherms were used to study the distribution of Cu^{2+} and MB molecules between solid hydrogels and aqueous phase at equilibrium. Cu^{2+} and MB adsorption data at equilibrium (q_e) for various initial feed adsorbates concentrations (C_e) were fitted to the following two-parameter Langmuir and Freundlich (Eqs. (4 and 5), respectively) isothermal models. However, the adsorption data for both adsorbates were not found to give

good fits to either of these two models. Therefore, a new switch model, that is, from a Freundlich to Langmuir isotherm, was used to analyze the adsorption isotherms of MB:

$$\frac{c_e}{q_e} = \frac{1}{q_{\max} K_L} + \frac{c_e}{q_{\max}} \tag{4}$$

$$\ln q_e = \ln K_F + \frac{\ln c_e}{n} \tag{5}$$

where q_{max} is the maximum monolayer adsorption, k_L and k_F are Langmuir and Freundlich constants, and n is a parameter concerning the Freundlich model.

Thermodynamic parameters

The thermodynamic distribution coefficient, K_d [19], was obtained from the Cu^{2+} and MB adsorbed at equilibrium (q_e) and the equilibrium feed adsorbates concentration, C_e, as:

$$K_d = \frac{q_e}{c_e} \tag{6}$$

The change in standard Gibbs energy (ΔG^θ) is also related to K_d, as

$$\Delta G^\theta = -RT \ln K_d \tag{7}$$

Further:

$$\ln K_d = \frac{\Delta S^\theta}{R} - \frac{\Delta H^\theta}{RT} \tag{8}$$

where ΔH^θ and ΔS^θ are changes in standard enthalpy and entropy, respectively.

Results and discussion

Synthesis of casein hydrogels

Owing to the Schiff-base crosslinking between the amino groups in casein and the aldehyde groups in glutaraldehyde, aqueous casein solution (10.0 wt%) was transformed into a hydrogel when aqueous solution of glutaraldehyde (2.5–10 wt%) was introduced, as shown in Fig. 1. Similar gelation phenomena have also been reported for mixed aqueous systems composed of casein and oxidized hyaluronic acid [9]. Moreover, there was a clear color change from light yellow to deep red when the aqueous casein solution was gelled in the presence of glutaraldehyde. We attributed this result to the formation of Schiff-base links between the free amino groups of casein and the aldehyde groups of glutaraldehyde, as shown in Fig. 1 [20–22]. The resultant hydrogel sample with 10 wt% casein and 5 wt% crosslinker is denoted C10 and was characterized by Fourier transform infrared (FTIR) spectroscopy, thermogravimetric analysis (TGA), and adsorption testing.

Characterization of the hydrogels

FTIR spectroscopy

The FTIR spectra of the casein powder and the hydrogel sample C10 with 10 wt% casein and 5 wt% crosslinker are shown in Fig. 2. The stretching vibration of the amide carbonyl group of casein at 1624 cm^{-1} shifted to higher frequencies (i.e., 1633 and 1638 cm^{-1}) for the casein gel. This shift of the amide carbonyl groups of casein to a higher frequency indicated the formation of C=N bonds owing to crosslinking. A new peak at 970 cm^{-1} corresponds to the C-H *trans* bending vibration of the –CH=N group, and the shift of the stretching vibration of the C-N group from 1076 to 1093 cm^{-1}, confirmed the Schiff base formation, as shown in Fig. 1.

TGA results

The TGA curves of the casein powder and its gel C10 are shown in Fig. 3. Both curves were similar, indicating that there was no obvious differences in the thermal stability of casein and its crosslinked gel. Below 150 °C, both samples lost approximately 10% of their weight, which we attributed to be loosely bounded water molecules in the samples. Below 200 °C, both samples had a 10%-weight loss, indicating their good thermal stability. Above 210 °C, both samples started to lose weight, and were completely decomposed at approximately 500 °C.

SEM analysis

The surface morphology of the casein gels with different contents of crosslinker and casein are respectively shown in Figs. 4 and 5. The images in the first row of Fig. 4 show the rough surface of the casein powder, which had a large block structure. The surfaces of the four kinds of casein hydrogels with different contents of crosslinker from the second row to the fifth row in Fig. 4 were smooth, and many lamella and network structures appeared as the content of crosslinker was increased. In particular, we observed that the hydrogel sample with 5.0 wt% crosslinker in the fourth row had the most uniform network structure. Hydrogels with a

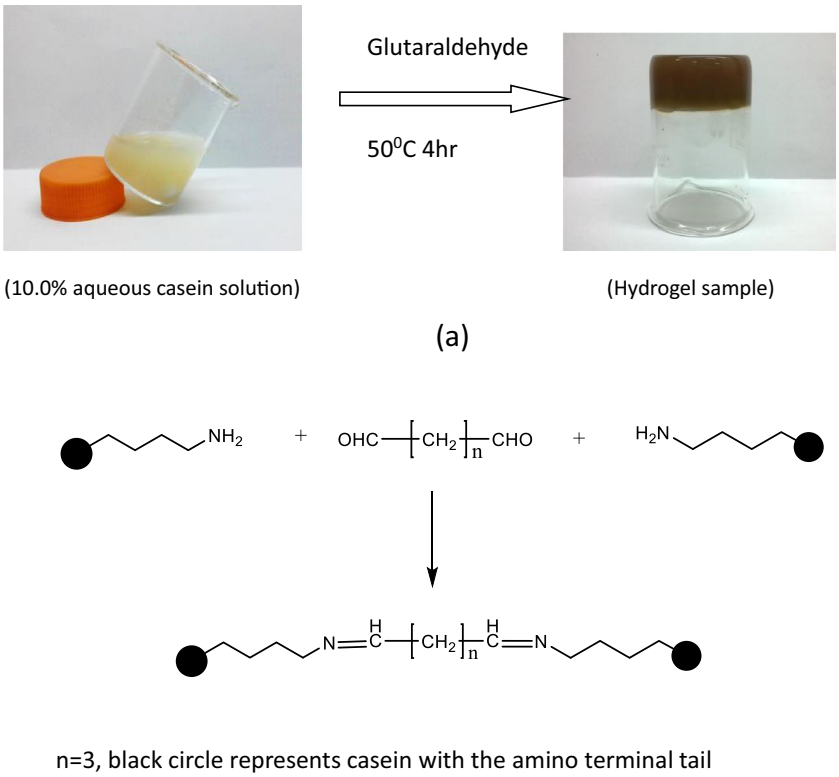

Fig. 1 Photographs for the casein hydrogel formation when 10.0% aqueous casein solution was mixed with 5% aqueous glutaraldehyde solution (**a**) and a graphical representation for Schiff's base crosslinking reaction involved (**b**)

similar surface morphology were observed for different contents of casein (Fig. 5). The hydrogel sample with 10.0 wt% casein and 5 wt% glutaraldehyde (C10), in the third row of Fig. 5, had the most uniform network structure. This C10 sample had a good adsorption capacity for Cu^{2+} and methylene blue (MB). The SEM images showed some cracks and a few pore structures. The phase morphology became coarser as the amount of casein was increased (Fig. 5).

Cu^{2+} and MB adsorption

Effects of glutaraldehyde content on Cu^{2+} and MB adsorption

The Cu^{2+} and MB were adsorbed into the hydrogel sample in adsorption experiments. The Cu^{2+} and MB adsorption capacities (q_e, mg.g^{-1} of gel) of the four hydrogels with different glutaraldehyde contents (2.5%, 3.5%, 5.0%, and 10%) are shown in Fig. 6. Because the adsorption

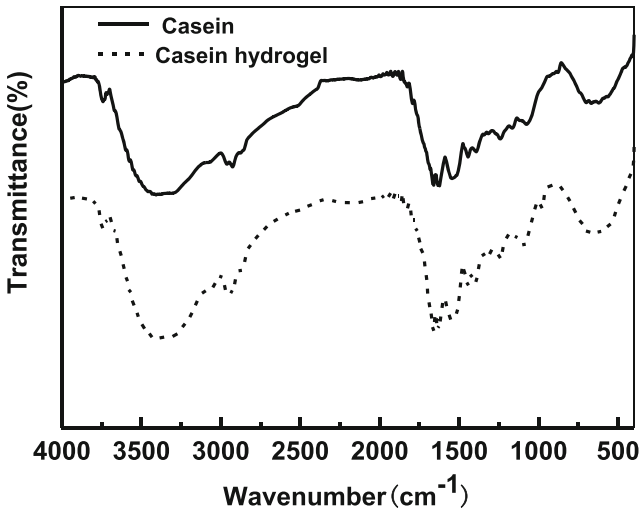

Fig. 2 FTIR spectra of casein powder and the C10 hydrogel

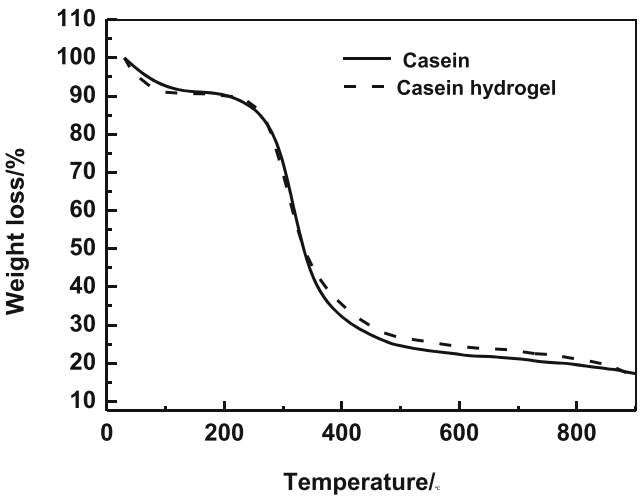

Fig. 3 TGA curves of casein powder and the C10 hydrogels

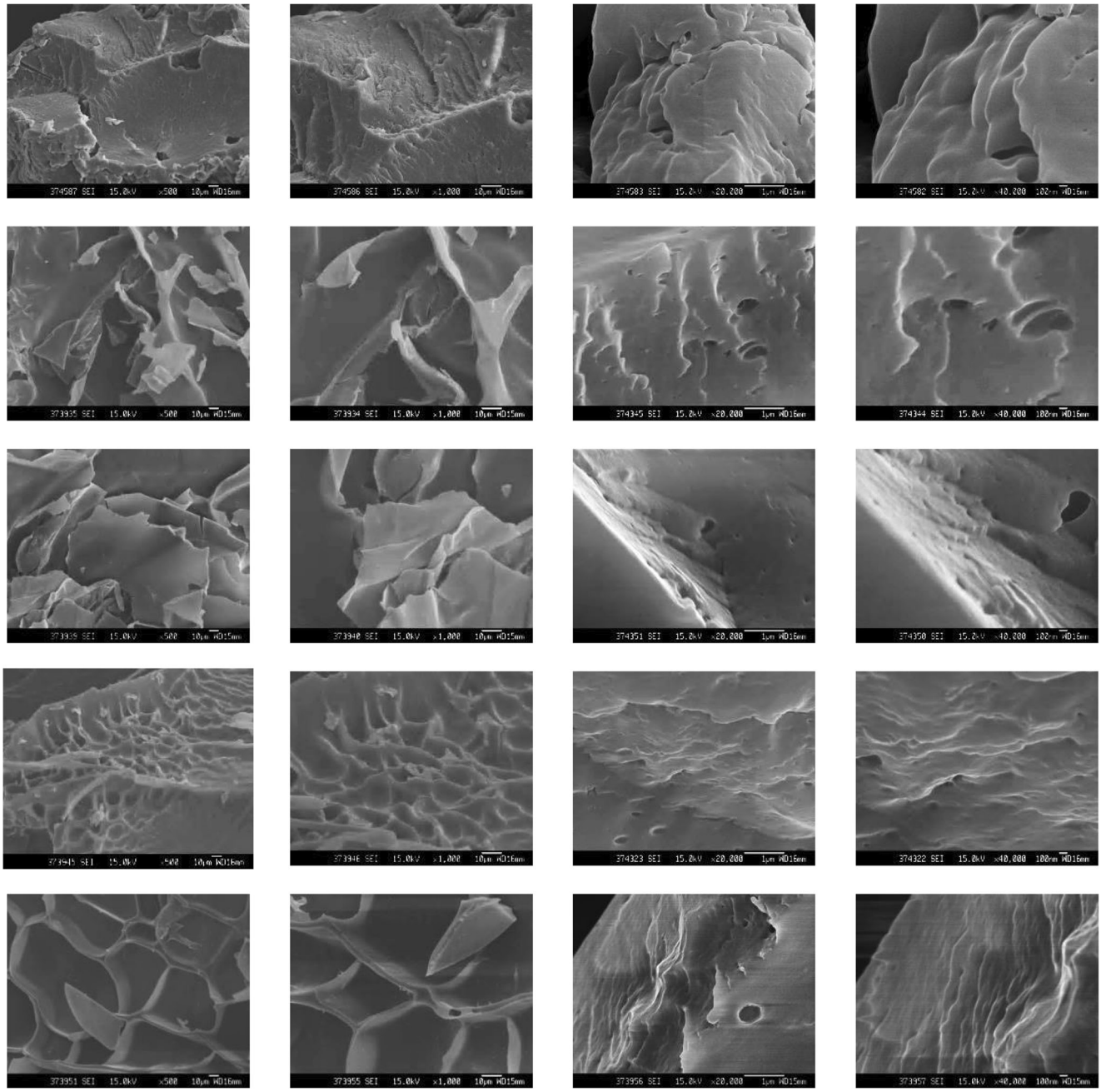

Fig. 4 SEM images of casein powder and the four kinds of casein hydrogels with different contents of crosslinker (From top to bottom: casein powder and the hydrogels with 10 wt% of casein and different glutaraldehyde contents of 2.5, 3.5, 5.0 and 10.0 wt% respectively; From left to right: magnification factors of samples are 500, 1000, 20,000 and 40,000, respectively)

capacity was affected by the feed concentration of Cu^{2+} and MB, in this experiment, the feed concentrations of Cu^{2+} and MB were selected to be 50 and 100 mg/L respectively, which are the intermediate feed concentrations. Figure 6a shows that the adsorption capacity of Cu^{2+} into the hydrogels increased at first and then decreased as the glutaraldehyde content was increased. The hydrogel with 5% glutaraldehyde had the highest adsorption capacity for Cu^{2+}. Chelation effects and electrostatic interactions between the casein hydrogel and Cu^{2+} ions increased with increasing glutaraldehyde content up to 5.0%. However, when the content of crosslinker was greater than 5.0%, the specific surface area of the casein hydrogel decreased and the carbonyl functional groups participating in the reaction was also reduced, which lowered the adsorption capacity. The adsorption capacity of the hydrogel for MB increased as the glutaraldehyde contents increased over the whole glutaraldehyde concentration range of

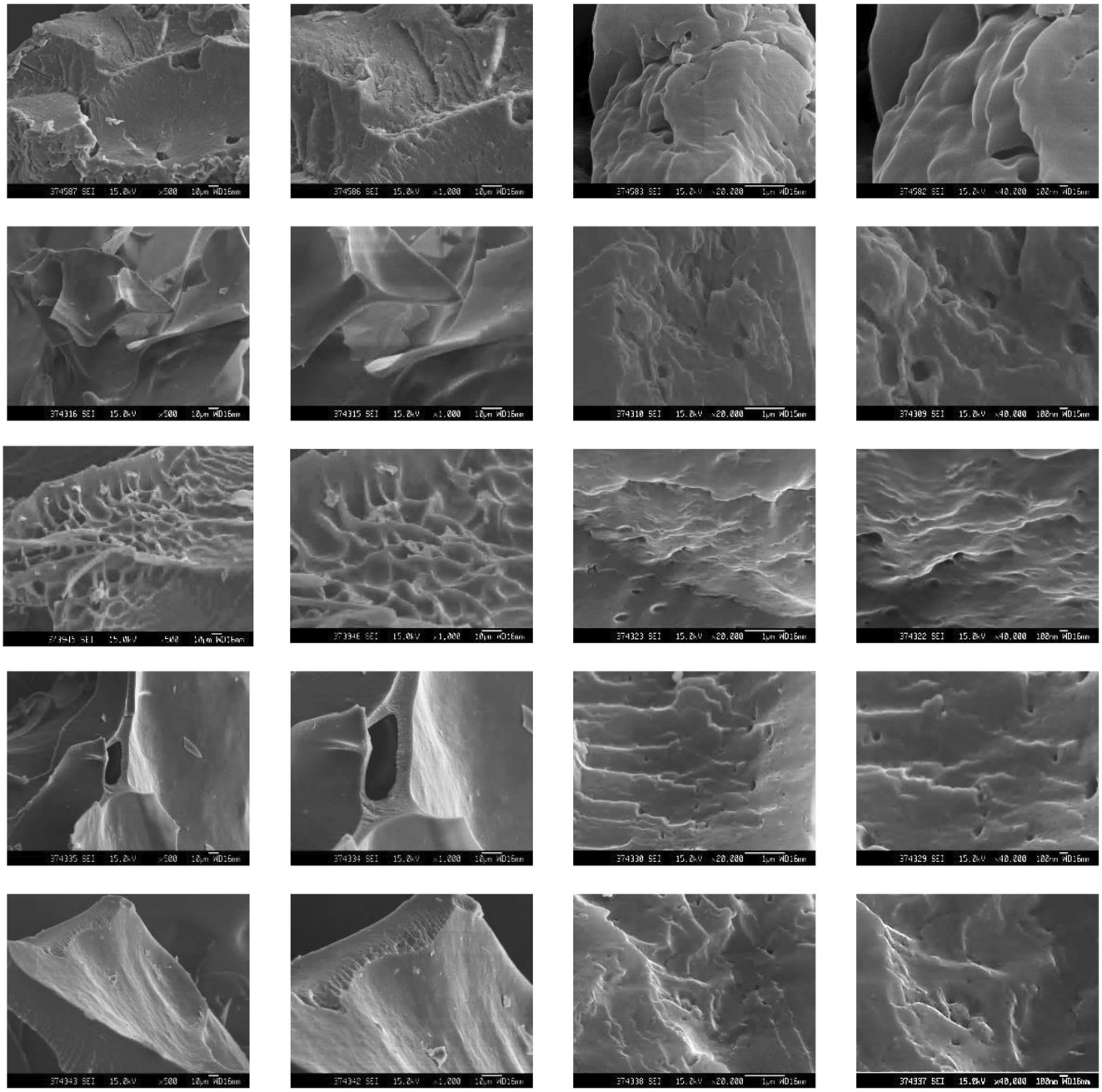

Fig. 5 SEM images of casein powder and the four kinds of casein hydrogels with different contents of casein (From top to bottom: casein powder and hydrogels with 5 wt% of glutaraldehyde and different casein contents of 8.0, 10.0, 12.0 and 14.0 wt%, respectively; From left to right: magnification factors of samples are 500, 1000, 20,000 and 40,000, respectively)

2.5%–10% (Fig. 6b). Because MB is a cationic dye and contains tertiary amine groups, the strong electrostatic interactions and hydrogen bonding between the casein hydrogel and MB molecules favored MB adsorption over the whole range of glutaraldehyde contents.

Effects of casein content on Cu^{2+} and MB adsorption

The Cu^{2+} and MB adsorption capacities of the four hydrogels with various casein contents (8.0%, 10.0%, 12.0%, and 14.0%) are shown in Fig. 7. The feed concentrations of Cu^{2+} and MB were selected to be 50 and 100 mg/L, respectively. The adsorption capacity of the hydrogels for Cu^{2+} decreased as the casein contents increased, whereas the adsorption capacity of the hydrogel for MB increased as the casein contents were increased over the range of 8.0%–14.0%. We attribute this behavior to the specific surface area of the hydrogel decreasing as the casein content was increased. At higher casein contents, a more compact hydrogel structure was

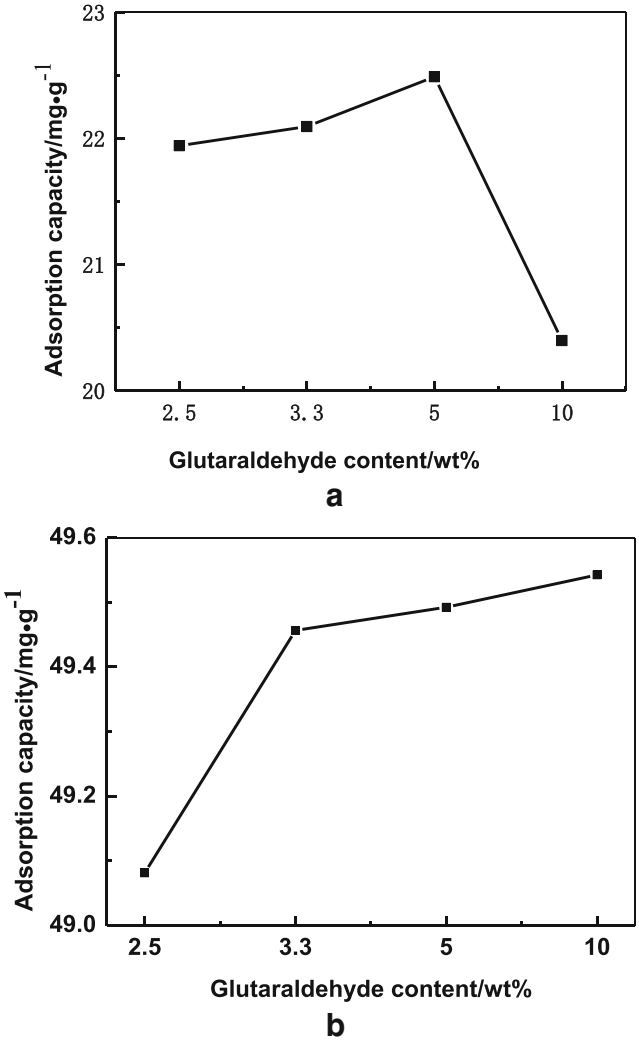

Fig. 6 The effect of glutaraldehyde content on Cu^{2+} (**a**) and MB dye (**b**) adsorption for the casein hydrogels with different glutaraldehyde contents

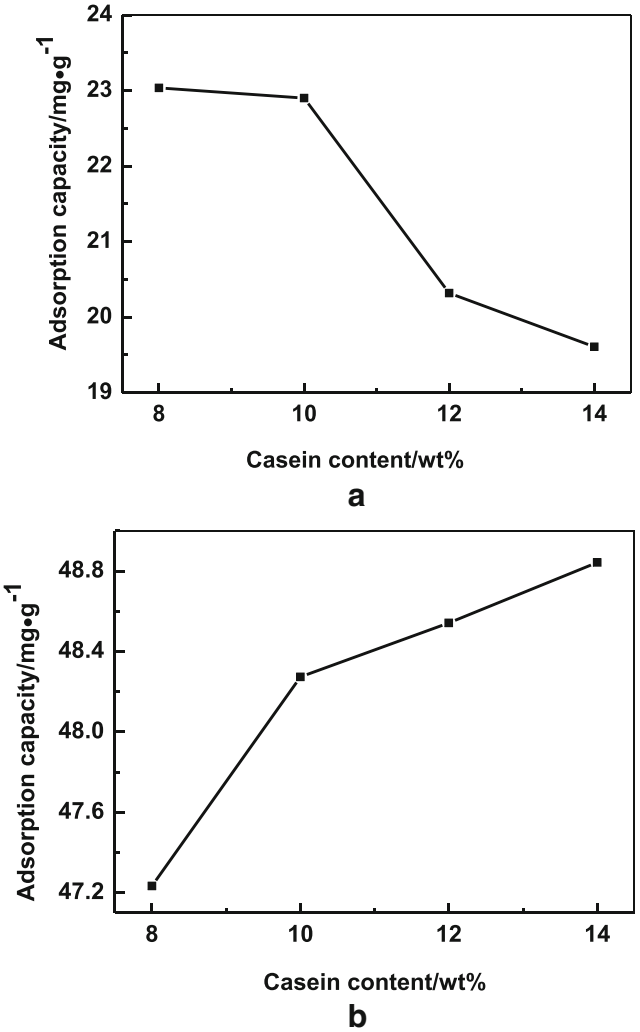

Fig. 7 The effect of casein content on Cu^{2+} (**a**) and MB dye (**b**) adsorption for the casein hydrogels with different casein contents

produced, which was not conducive to the attachment of Cu^{2+}. For MB adsorption, strong electrostatic interactions and hydrogen bonds between casein hydrogel and MB molecules favored MB adsorption over the whole range of casein concentrations.

Effect of feed concentration on Cu^{2+} and MB adsorption

Typically, a fixed amount of hydrogel can absorb a fixed amount of dye molecules. As the feed concentration increases, this fixed amount decreases [23]. The results of Cu^{2+} and MB adsorption onto a C10 hydrogel at room temperature for both a low (10–150 mg/L) and high (50–500 mg/L) range of feed concentrations of Cu^{2+} and MB are shown in Fig. 8. The Cu^{2+} adsorption monotonously increased over the feed concentration range of 10–50 mg/L and then gradually increased and reached equilibrium as the feed concentration was increased from 50 to 150 mg/L for C10 hydrogel (Fig. 8a). The casein hydrogel featured a sufficient number of adsorption sites when the concentration of Cu^{2+} was low. Hence, as the concentration of Cu^{2+} was increased from 10 to 50 mg/L, the adsorption of Cu^{2+} into C10 hydrogel became easier and the amount adsorbed rapidly increased. However, when the concentration of Cu^{2+} increased to approximately 80 mg/L, the adsorption sites of casein hydrogel became occupied and adhesion of Cu^{2+} was decreased, resulting a saturated adsorption. The C10 hydrogel showed very high adsorption for Cu^{2+} and a maximum q_e of 25.4 $mg.g^{-1}$ was observed over the feed concentration of 10–150 $mg.L^{-1}$. For MB adsorption, we observed from Fig. 8b that the adsorption capacity of the hydrogel for MB increased for a feed concentration over the whole feed concentration range of 50–500 $mg.L^{-1}$, and a maximum q_e of 241.4 $mg.g^{-1}$ was achieved. This is because strong electrostatic interactions between functional groups of MB and the hydrogel contributed to strong adsorption of MB.

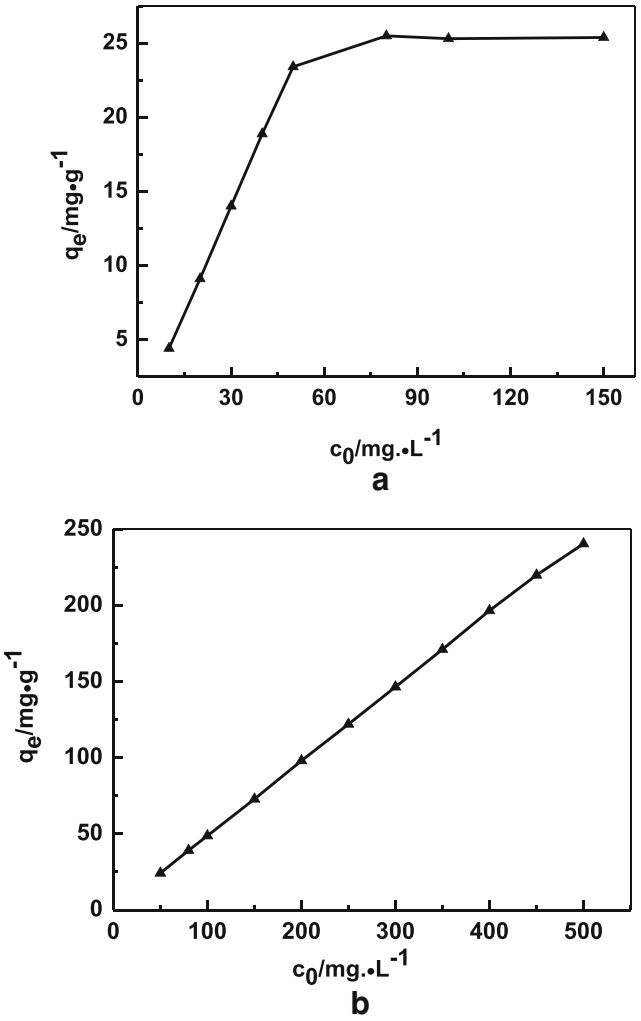

Fig. 8 The effect of feed concentration on Cu^{2+} (**a**) and MB (**b**) adsorption into the C10 hydrogel at room temperature

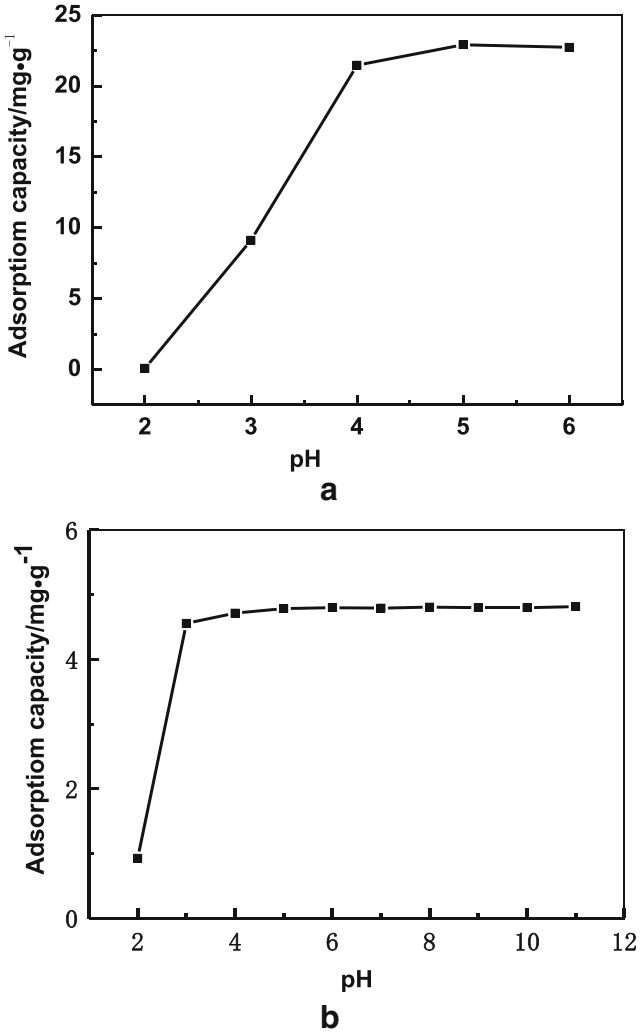

Fig. 9 The effect of pH value on Cu^{2+} (**a**) and MB dye (**b**) adsorption by the C10 hydrogel at room temperature

Effects of pH on Cu^{2+} and MB adsorption

The effects of initial pH on the adsorption of Cu^{2+} and MB at equilibrium on the casein hydrogels at 15, 20, and 25 °C, are shown in Fig. 9. The pH of the heavy metal ion solution strongly influenced the sorption process because metal speciation and the surface charge of the sorbent are highly dependent on pH [24, 25]. In this work, we investigated the effect of solution pH on the amounts of Cu^{2+} and MB adsorbed at equilibrium by varying the initial pH in the range 2.0–6.0 and 2.0–11.0 respectively, with other parameters held constant. As shown in Fig. 9a, when the initial pH of Cu^{2+} solution increased from 2.0 to 4.0, the amount of Cu^{2+} absorbed at equilibrium monotonously increased, and reached equilibrium when pH increased up to 6.0 for C10 hydrogel. This is because at low pH (pH 2), competition between H^+ and Cu^{2+} ions for the same active sites (i.e., carbonyl and amine groups in casein) favored protonation of the carbonyl groups and amine in the casein hydrogel surface and decreased the amount of Cu^{2+} ions absorbed into the hydrogel at this pH. As the pH was increased from 2.0 to 4.0 the Cu^{2+} sorption capacity increased because the degree of protonation of carbonyl and amine groups decreased, and the surface became less positive. Interactions such as ion-exchange and chelation between Cu^{2+} ions and the sorbent surface were thus strengthened [24, 25]. Further increases of the pH from 4.0 to 6.0 adversely affected the Cu^{2+} sorption equilibrium because the concentration of OH^- ions was sufficiently high to interact with Cu^{2+}, which thus reduced the availability of Cu^{2+} in its free form. When the initial pH of the MB solution was increased from 2.0 to 3.0, the amount of MB absorbed at equilibrium monotonously increased, and then saturated when the pH was increased to 11.0 for the C10 hydrogel (Fig. 9b). We attribute this result to steric hindrance and electrostatic repulsion between the absorbed MB absorbed.

Effects of contact time and temperature on Cu^{2+} and MB adsorption

The effects of contact time and temperature on Cu^{2+} and MB adsorption into C10 are shown in Fig. 10. The feed concentrations of Cu^{2+} and MB were selected to be 50 and 100 mg/L respectively. Both Cu^{2+} and MB adsorption monotonously increased and reached equilibrium within approximately 30 min for the C10 hydrogel. Dye adsorption by hydrogels is governed by diffusion of dye molecules from the solution to the surface of the hydrogels followed by pore diffusion into the interior of the hydrogel [16]. The transport of dye molecules from the bulk feed to the surface of the hydrogel occurred by diffusion, which transferred the molecules from the surface to the interior of gel. Hence, mass transfer resistance at the interface between the feed and hydrogel surface is important. At higher feed dye concentrations, the mass transfer resistance for transport of dye molecules is reduced, which leads to a shorter equilibrium time [23, 26]. Therefore, the MB adsorption equilibrium with a high feed concentration of 100 $mg.L^{-1}$ at 313 K occurred within approximately 30 min, whereas the Cu^{2+} adsorption equilibrium at a low feed concentration (50 $mg.L^{-1}$) of Cu^{2+} at 313 K required approximately 60 min. Hence, a higher feed concentration gave a faster adsorption rate. Additionally, stronger interactions between MB and casein hydrogel than between Cu^{2+} and the casein hydrogel also promoted adsorption of MB. The amount of adsorption at equilibrium for C10 respectively reached 49.10, 49.14, and 49.19 $mg{\cdot}g^{-1}$ at 308, 313, 318 K for MB; and 21.9, 22.9, and 23.4 $mg{\cdot}g^{-1}$ at 303, 313, and 323 K for Cu^{2+}. Both Cu^{2+} and MB adsorption capacities and rates at high temperature (318 K) were greater than those at low temperature (308 K), indicating that high temperatures favored Cu^{2+} and MB adsorption over the range of 308–318 K. This result is also in agreement with the later thermodynamic experimental results, which indicated that both the Cu^{2+} and MB adsorption process are endothermic.

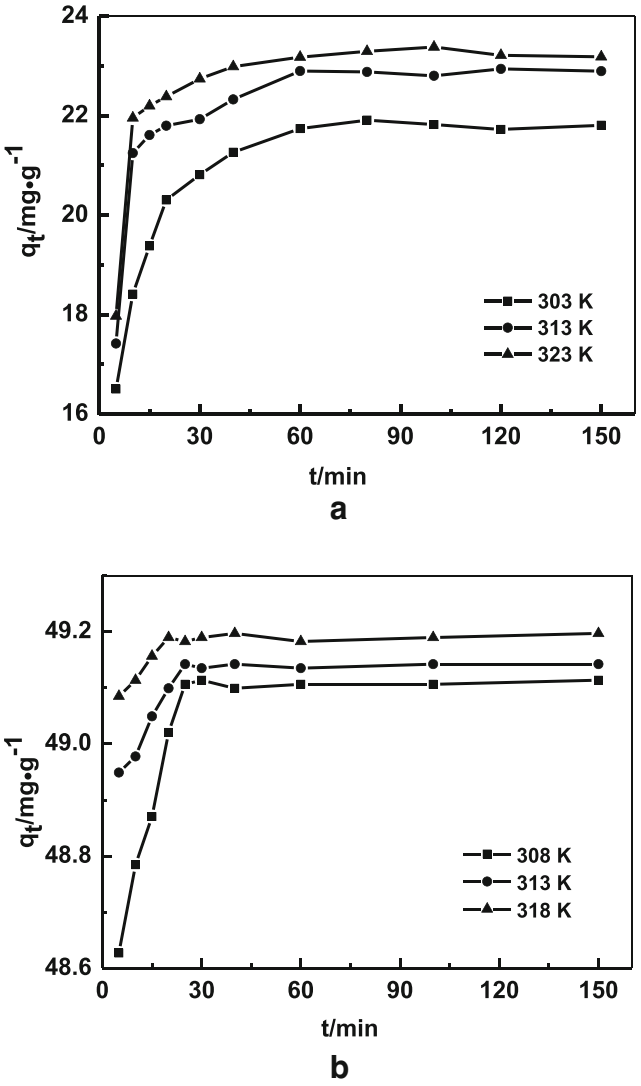

Fig. 10 The effect of contact time and temperature on Cu^{2+} (**a**) and MB (**b**) adsorption into the C10 hydrogel at different temperatures

Fitting of Cu^{2+} and MB adsorption data to adsorption kinetics

The linear fitting results of Cu^{2+} and MB adsorption data to pseudo second order kinetics equation are shown in Fig. 11 and Table 1. Both the Cu^{2+} and MB adsorption data (q_t) at various time intervals (t) were well fitted to a pseudo second order rate equation (Eq. 2). The calculated equilibrium adsorption value (q_2) in Table 1 based on the pseudo second order kinetics was close to the experimental equilibrium value. The statistical parameters for these adsorption results are shown in Table 1. The R^2 values for the fits were close to unity confirming the close fit of the data to the model. Good fitting of Cu^{2+} and MB adsorption data to the pseudo second order kinetics also confirmed a mechanism involving chemical adsorption through electrostatic interactions between the Cu^{2+} or MB molecules and hydrogels as the rate determining step [27]. In the present system, the Cu^{2+} and MB adsorption data were poorly fitted by pseudo 1st order rate kinetics and these results are not shown.

The mechanism of diffusion of Cu^{2+} and MB from water to the hydrogel was explained by fitting of the adsorption data (q_t) at the square root of various time intervals ($t^{1/2}$) to the intra particle diffusion model (Eq. 3), as shown in Fig. 12. The intra particle fits showed multiple regions of linearity, which indicated various different mechanisms for Cu^{2+} and MB adsorption. The first linear region corresponded to rapid external surface adsorption by boundary layer diffusion of adsorbates whereas the second region corresponds to intra particle diffusion. Equilibrium adsorption was achieved in the third and final slow stage. None of the lines passed through the origin and the values of the intercept are related to thickness of the boundary layer. The values of k_p (rate constant) and C

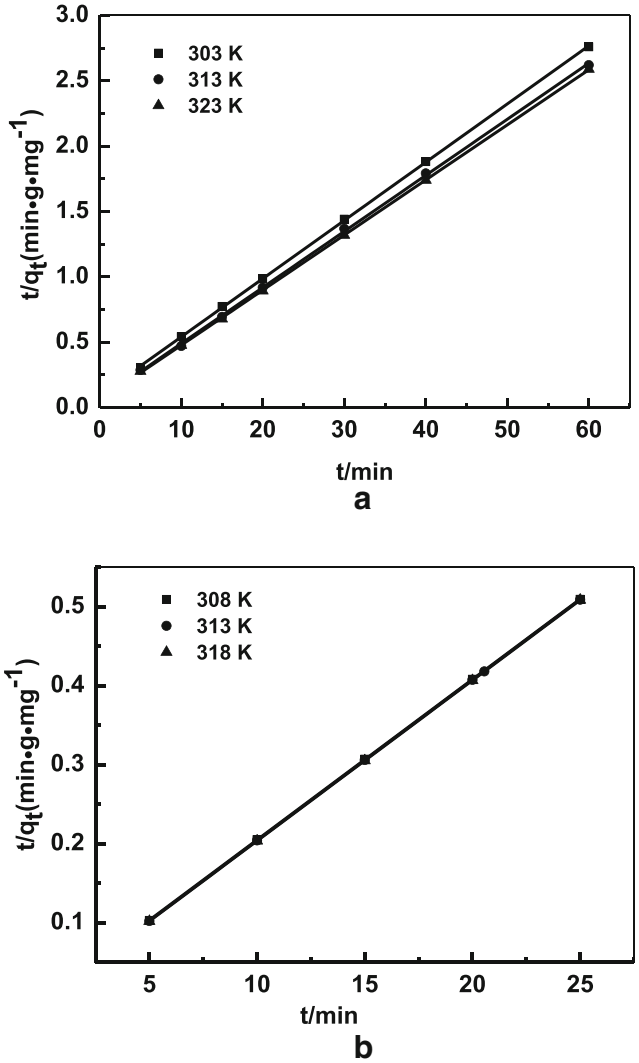

Fig. 11 Linear fitting of adsorption data of Cu^{2+} (**a**) and MB (**b**) to Ho and McKay pseudo second order kinetics

(intercept), and the statistical parameters, i.e., the R_p^2 values for the second phase (stage 1) and third phase (stage 2) of the linear region are listed in Table 2. The rate constant (k_p) for Cu^{2+} adsorption in stage 1 also increased with increasing temperature from 303 to 313 K, and the intercept (C) decreased with increasing temperature, indicating that a higher temperature favored faster diffusion owing to a decrease in the thickness of boundary layer at stage 1 [28]. Furthermore, in stage 2, the rate constant (k_p) for Cu^{2+} adsorption decreased as the temperature was increased from 303 to 313 K, and the intercept (C) increased with increasing temperature. Thus, higher temperatures made diffusion unfavorable owing to a decrease of the Cu^{2+} concentration in the solution and an increase in the thickness of boundary layer. Similar results to the Cu^{2+} adsorption in stage 2 were found for MB adsorption in stage 1 and the parameters are listed in Table 2. Therefore, both the Cu^{2+} and MB adsorption data fitted well with intra particle diffusion model, indicating that the initial adsorption rates of Cu^{2+} and MB were well controlled by external mass transfer. At a later stage, the overall rates of adsorption were controlled by intra particle diffusion [19].

Fitting of Cu^{2+} and MB adsorption data to adsorption isotherms

The equilibrium Cu^{2+} and MB adsorption data (q_e) into C10 hydrogel at various feed concentrations (C_e) were fitted to the Langmuir and Freundlich models. The Langmuir isotherm assumes homogeneous adsorption sites in the hydrogels with negligible interactions among the adsorbed molecules. The Freundlich isotherm is related to the surface heterogeneity. The fitting results for Cu^{2+} and MB adsorption based on single-layer Langmuir or single-layer Freundlich models were unsuitable because of the low correlation coefficient (R^2) of the fitting and negative slope values. Therefore, a Freundlich–Langmuir switch model was used to analyze the adsorption isotherms of Cu^{2+} and MB. The fitting results of Cu^{2+} and MB adsorption data to Freundlich–Langmuir switch model are shown in Fig. 13 and Table 2. The adsorption isotherm data was well simulated first by the Freundlich isotherm up to the switch point and then by Langmuir isotherm after the switch point (Fig. 13a and Fig. 13b). All the switch points are indicated by circles in Fig. 13. The improved correlation coefficients and statistical parameters are shown in Table 2, and also indicated favorable adsorption by this isotherm. The maximum adsorption capacities of casein hydrogel calculated from Freundlich–Langmuir switch model isotherms were respectively found to be 24.77, 25.48, 25.48 $mg.g^{-1}$ at 303, 313, and 323 K for Cu^{2+}, which were close to the

Table 1 Fitting results of MB and Cu^{2+} adsorption data to pseudo second order kinetics equation

T/K	MB			Cu^{2+}		
	$k_2(min^{-1})$	$q_2(mg{\cdot}g^{-1})$	R_2^2	$k_2(g{\cdot}mg^{-1}{\cdot}min^{-1})$	$q_2(mg{\cdot}g^{-1})$	R_2^2
303	0.24	49.23	0.9999	0.021	22.45	0.9998
313	0.56	49.19	1	0.030	23.31	0.9996
323	1.20	49.21	1	0.032	23.72	0.9999

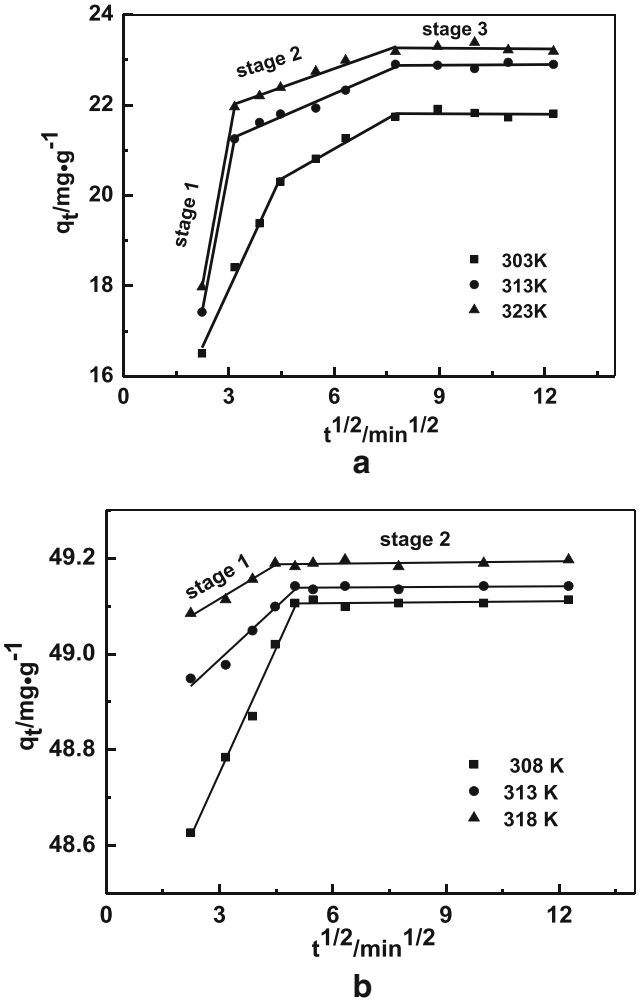

Fig. 12 Fitting results of Cu2+ (**a**) and MB (**b**) adsorption data at different temperatures to intra particles diffusion model

experimental results. The experiments showed a maximum q_e of 25.4 mg.g $^{-1}$ over the feed concentration of 10–150 mg/L for Cu^{2+} at room temperature. The maximum adsorption capacities of casein hydrogel calculated from Freundlich–Langmuir switch model isotherms for MB were respectively 395.26, 333.33, and 284.09 mg·g^{-1} at 308, 313, and 318 K, which were slightly higher than the experimental values at room temperature. The maximum q_e of 241.4 mg·g $^{-1}$ was observed over the feed concentration of 10–150 mg·L^{-1} for MB at room temperature. Furthermore, we infer that the new Freundlich–Langmuir switch model gives a closer fit to the actual adsorption behavior of Cu^{2+} and MB into the casein hydrogels. When the initial adsorbate concentration was low, the isothermal adsorption of the casein hydrogel followed the Freundlich model; when the adsorbate concentration was high, the isothermal adsorption followed the Langmuir model. We regarded the switch point from the Freundlich to Langmuir isotherm as the change from exponential adsorption to single layer adsorption, which is the point at which the increase of the equilibrium adsorption capacity was unable to keep pace with the increase of the equilibrium concentration (Table 3).

Effects of temperature on Cu^{2+} and MB adsorption and thermodynamic parameters

The changes in standard Gibbs energy ($\Delta G^{\ominus}$), standard enthalpy ($\Delta H^{\ominus}$) and standard entropy ($\Delta S^{\ominus}$) for Cu^{2+} and MB adsorption were obtained using Eqs. (6–8). The thermodynamic distribution coefficient K_d at three different temperatures was determined

Table 2 Fitting results of Cu^{2+} and MB and adsorption data at different temperatures to intra particle diffusion model

Cu^{2+} / T/K	k_p(mg·g^{-1}·min$^{-1/2}$)		C(mg·g^{-1})		R_p^2	
	Stage 1	Stage 2	Stage 1	Stage 2	Stage 1	Stage 2
303	1.68	0.44	12.87	18.38	0.9861	0.9806
313	4.14	0.34	8.17	20.22	-	0.9722
323	4.30	0.28	8.35	21.14	-	0.9644

MB / T/K	Stage 1		
	k_p(mg·g^{-1}·min$^{-1/2}$)	C(mg·g^{-1})	R_p^2
308	0.17	48.23	0.9870
313	0.07	48.77	0.9562
318	0.05	48.97	0.9660

Table 3 Fitting results of Cu^{2+} and MB and adsorption data at different temperatures to Freundlich-Langmuir switch model

Cu^{2+} / T/K	Before switch point(Freundlich)			After switch point(Langmuir)		
	K_F (mg·g^{-1})	1/n	R^2	q_{max} (mg·g^{-1})	K_L(L·g^{-1})	R^2
303	2.48	1.90	0.9948	24.77	1.54	0.9999
313	3.54	2.60	0.9598	25.48	2.11	0.9999
323	3.49	2.87	0.9642	25.48	2.99	0.9999
MB / T/K	Before switch point(Freundlich)			After switch point(Langmuir)		
	K_F (mg·g^{-1})	1/n	R^2	q_{max} (mg·g^{-1})	K_L (L·g^{-1})	R^2
308	16.24	1.40	0.9902	395.26	0.11	0.9948
313	19.45	1.21	0.9968	333.33	0.14	0.9940
318	19.35	1.21	0.9964	284.09	0.33	0.9999

from Cu^{2+} and MB adsorption with the use of Eq. (6). The values of $\Delta H^{\ominus}$ and $\Delta S^{\ominus}$ were respectively determined from the slope and intercept of linear plots of lnK_d versus 1/T. Both Cu^{2+} and MB adsorption capacities increased at higher temperatures, as shown in Fig. 10, indicating the endothermic nature of the adsorption. The values of $\Delta G^{\ominus}$ at the three temperatures for Cu^{2+} and the MB adsorption process are given in Table 4. Negative values of $\Delta G^{\ominus}$ confirmed the feasibility and spontaneity of the Cu^{2+} and MB adsorption process. Positive $\Delta S^{\ominus}$ values for adsorption of both species, as listed in Table 4, indicate an

Table 4 Thermodynamic parameters of Cu^{2+} and MB adsorption into casein hydrogel

Cu^{2+} / T/K	ΔH^{θ}(kJ·mol^{-1})	ΔS^{θ}(J·mol^{-1}·K^{-1})	ΔG^{θ}(kJ·mol^{-1})
303			-5.50
313	41.68	155.76	-7.10
323			-8.61
MB / T/K	ΔH^{θ}(kJ·mol^{-1})	ΔS^{θ}(J·mol^{-1}·K^{-1})	ΔG^{θ}(kJ·mol^{-1})
308			-8.48
313	7.38	51.46	-8.71
318			-9.00

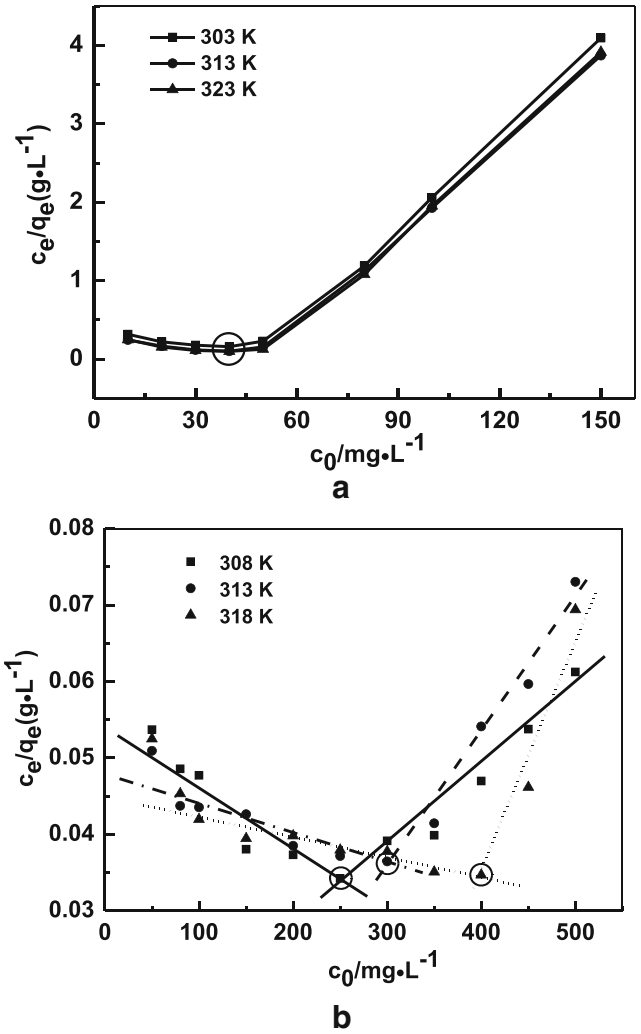

Fig. 13 C_e/q_e vs.C_0 curves of adsorption isotherm using Freundlich-Langmuir switch model for Cu^{2+}(**a**) and MB (**b**) adsorption into the C10 hydrogel at different temperatures (the switch points are labelled by circles)

increase of randomness in the solid (gel)-adsorbate solution interface during adsorption. A positive $\Delta H^{\ominus}$ value also confirmed the endothermic nature of adsorption [29].

Conclusion

Several casein hydrogels were synthesized with the use of glutaraldehyde as a crosslinker. The hydrogel prepared from 10 wt% of casein and 5 wt% of glutaraldehyde solution at pH = 7.5 showed the best adsorption performance for Cu^{2+} and MB adsorption. The adsorption data showed that the adsorption processes of Cu^{2+} and MB into the casein hydrogel was spontaneous chemisorption. This casein hydrogel is a promising absorbent material owing its high adsorption rate and good adsorption capacity.

Acknowledgments This work was supported by the Key project of Guangdong Natural Science Foundation of China (2017B030311007), the Special Funds for Public Welfare Research and Capacity Building of Guangdong Province in China (2016A020222017), and the Science and Technology Planning Project of Guangzhou, Guangdong Province, China (201607010249).

References

1. Carmalin Sophia A, Lima EC (2018) Removal of emerging contaminants from the environment by adsorption. Ecotoxicol Environ Saf 150:1–17
2. GilPavas E, Dobrosz-Gomez I, Gomez-Garcia MA (2019) Optimization and toxicity assessment of a combined electrocoagulation, H2O2/Fe2+/UV and activated carbon adsorption for textile wastewater treatment. Sci Total Environ 651:551-560
3. Senthilkumar K, Devi VC, Mothil S (2018) Adsorption studies on treatment of textile wastewater using low-cost adsorbent. Desalin Water Treat 123:90-100
4. Ni N, Zhang D, Dumont MJ (2018) Synthesis and characterization of zein-based superabsorbent hydrogels and their potential as heavy metal ion chelators. Polymer Bulletin (1):31–45
5. Shi W, Dumont MJ, Ly EB (2014) Synthesis and properties of canola protein-based superabsorbent hydrogels 54:172–180
6. Wattie B, Dumont MJ, Lefsrud M (2018) Synthesis and Properties of Feather Keratin-Based Superabsorbent Hydrogels. Waste Biomass Valoriz 9:391–400
7. Li N, Fu C, Zhang L (2014) Using casein and oxidized hyaluronic acid to form biocompatible composite hydrogels for controlled drug release. Mater Sci Eng C36:287–293
8. Fox PF, Mulvihill DM, Harris P (1990) Food gels, Elsevier Applied Science, London
9. AJE F, Teller SS, Jha AK, Jiao T, Hule RA, Clifton RJ, Pochan DP, Duncan RL, Jia X (2010) Effects of Matrix Composition, Microstructure, and Viscoelasticity on the Behaviors of Vocal Fold Fibroblasts Cultured in Three-Dimensional Hydrogel Networks. Tissue Eng A16:1247–1261
10. Kundu J, Poole-Warren LA, Martens P, Kundu SC (2012) Silk fibroin/poly(vinyl alcohol) photocrosslinked hydrogels for delivery of macromolecular drugs. Acta Biomater 8:1720–1729
11. Abbate V, Kong X, Bansal SS (2012) Photocrosslinked bovine serum albumin hydrogels with partial retention of esterase activity. Enzyme Microb Technol 50:130–136
12. Amruthwar SS, Janokar AV (2012) Preparation and characterization of elastin-like polypeptide scaffolds for local delivery of antibiotics and proteins. J Mater Sci: Mater Med 23:2903–2912
13. Elzoghby AO, Abo El-Fotoh WS, Elgindy NA (2011) Casein-based formulations as promising controlled release drug delivery systems. J Controlled Release 153:206–216
14. Xu J, Fan Z, Duan L, Gao G (2018) A tough, stretchable, and extensively sticky hydrogel driven by milk protein. Polymer Chemistry 9:2617–2624
15. Koh LD, Cheng Y, Teng CP, Khin YW, Loh XJ, Tee SY, Low M, Ye E, Yu HD, Zhang YW, Han MY (2015) Structures, mechanical properties and applications of silk fibroin materials. Prog Polym Sci 46:86–110
16. Crini G (2008) Kinetic and equilibrium studies on the removal of cationic dyes from aqueous solution by adsorption into a cyclodextrin polymer. Dyes Pigm 77:415–426

17. Ho Y, McKay G (1999) Pseudo-second order model for sorption processes. Process Biochem 34:451–465
18. Weber W, Morris J, Sanit J (1963) Kinetics of adsorption on carbon from solution. Journal Sanitary Engeering Division Proceedings, vol 89. American Society of Civil Engineers, pp 31–60
19. Tang H, Zhou W, Zhang L (2012) Adsorption isotherms and kinetics studies of malachite green on chitin hydrogels. J Hazard Mater 209:218–225
20. Guinesi LS, ETG C (2006) Influence of some reactional parameters on the substitution degree of biopolymeric Schiff bases prepared from chitosan and salicylaldehyde. Carbohydrate Polymers 65: 557–561
21. Zhang R, Huang Z, Xue M, Yang J, Tan T (2011) Influence of some reactional parameters on the substitution degree of biopolymeric Schiff bases prepared from chitosan and salicylaldehyde. Carbohydr Polym 85:717–725
22. Hodge JE (1953) Chemistry of Browning Reaction in Model Systems. J Agric Food Chem 1:928–943
23. Bayramoglu G, Altintas B, Yakup AM (2009) Adsorption kinetics and thermodynamic parameters of cationic dyes from aqueous solutions by using a new strong cation-exchange resin. Chem Eng J 152:339
24. Guibal E (2004) Interactions of metal ions with chitosan-based sorbents: a review. Sep Purif Technol 38:43–74
25. Emik SM (2014) Preparation and characterization of an IPN type chelating resin containing amino and carboxyl groups for removal of Cu (II) from aqueous solutions. React Funct Polym 75:63–74
26. Bhattacharyya R, Ray SK (2014) Enhanced adsorption of synthetic dyes from aqueous solution by a semi-interpenetrating network hydrogel based on starch. J Ind Eng Chem 20:3714–3725
27. Al-Ghouti M, Khraisheh M, Ahmad SA (2005) Thermodynamic behavior and the effect of temperature on the removal of dyes from aqueous solution using modified diatomite: A kinetic study. J Colloid Interface Sci 287:6–13
28. Han X, Wang W, Ma X (2011) Adsorption characteristics of methylene blue into low cost biomass material lotus leaf. Chem Eng J 171:1–8
29. Anirudhan TS, Tharun AR (2012) Preparation and adsorption properties of a novel interpenetrating polymer network (IPN) containing carboxyl groups for basic dye from aqueous media. Chem Eng J 181:761–769